Analysis of the Microwave Spectrum of Tricarbon Oxide Sulfide, O=C=C=C=S, in Highly Excited Bending States

Manfred Winnewisser, E. Walter Peau *, and Koichi Yamada **
Physikalisch-Chemisches Institut der Justus-Liebig-Universität Giessen

and

Jørn Johs. Christiansen
Department of Chemistry, The Royal Danish School of Educational Studies, Copenhagen

Z. Naturforsch. **36a**, 819–830 (1981); received May 7, 1981

In memoriam Professor Dr. Werner Zeil

The microwave spectrum of tricarbon oxide sulphide (3-thioxo-1,2-propadiene-1-one), O=C=C=C=S, has been measured in the frequency range from 8 to 40 GHz and includes vibrational satellite lines arising from the vibrational manifold of the lowest-lying doubly-degenerate bending mode ν_7. The method of analysis followed the theory of rotation-vibrational interaction as developed by Nielsen and Amat. The spectroscopic constants B_v and D_v as well as several vibration-rotational constants for each vibrational state $v_7=0$ to 7, $v_5=1$ and $v_6=1$ were determined with the aid of a newly written least squares program. The program structure relies on the correlation of the symmetry classification of energy levels in linear and bent molecules, and follows closely the analysis of asymmetric rotor spectra. From the rovibrational spectrum of C_3OS in excited states of ν_7 up to $v_7=7$ and $l=6$ the sign and magnitude of the effective vibrational anharmonicity constant $x_{l_t l_t}$ were determined. The interpretation of these results yields the information that in C_3OS the potential function describing the two-dimensional oscillator of the ν_7 bending mode is very harmonic and does not contain a perturbing hump. The dynamic behaviour of C_3OS, a classical example of a linear molecule, is thus in sharp contrast to the quasilinear behaviour of C_3O_2.

I. Introduction

The pure rotational spectrum of 3-thioxo-1,2-propadien-1-one, O=C=C=C=S, was reported recently by Winnewisser and Christiansen [1]. The microwave spectrum of this molecule is that of a typical linear molecule and shows no sign of quasilinear behaviour. This is in sharp contrast to the complex infrared and submillimeter wave spectrum [2, 3] of O=C=C=C=O, which is almost half-way between a linear and a bent molecule [4, 5].

The molecule C_3OS has three degenerate bending modes which have first been estimated from relative intensity measurements [1] and were later confirmed by the infrared observations of Nicolaisen and Christiansen [6] to be $\nu_5=529\ cm^{-1}$, $\nu_6=429\ cm^{-1}$ and $\nu_7=77\ cm^{-1}$ (relative intensity estimate 83(10) cm^{-1}). Therefore the vibrational satellite lines in the pure rotational spectrum can be observed at room temperature from molecules in a large number of excited vibrational states. The energy levels of the ν_7 vibrational manifold are especially highly populated at room temperature, so that lines from states up to $v_7=18$ can be observed easily. In this paper we report our measurements and the analysis of C_3OS molecules in some of these vibrational states. A further publication will be concerned with the potential function of the ν_7 vibrational manifold as determined from relative intensity measurements of the reported vibrational satellite lines and the variation of the molecular electric dipole moment with the vibrational quantum number v_7 [7]. A third paper in this series will be concerned with the molecular structure of C_3OS [8].

II. Experimental Procedures

a) *Chemical Synthesis of C_3OS*

Samples of C_3OS were prepared by the reaction of C_3O_2 with P_4S_{10} as described in [1]. The experi-

* Present address: Institut für Atomphysik, Philipps-Universität Marburg, Renthof 5, D-3550 Marburg.

** Present address: I. Physikalisches Institut, Universität zu Köln, Universitätsstrasse 14, D-5000 Köln 41.

Reprint requests to Prof. Dr. Manfred Winnewisser, Physikalisch-Chemisches Institut, Justus-Liebig-Universität Giessen, Heinrich-Buff-Ring 58, D-6300 Giessen.

0340-4811 / 81 / 0800-0819 $ 01.00/0. — Please order a reprint rather than making your own copy.

mental set-up used in the preparation is shown in Figure 1. As can be seen from Figure 1, the synthesis of C_3OS starts with liquid C_3O_2 which is kept in a storage vessel at −40 °C. Its vapours are allowed to pass over a stirred, saturated aqueous solution of $CaCl_2$ at 20 °C in order to pick up a defined amount of water vapour. The substitution reaction of the replacement of oxygen in C_3O_2 by sulfur takes place in a U-tube (see Fig. 1) which contains a mixture of 10 g of a coarse fraction of Celite 545, 10 g of P_4S_{10} and 5 g of paraffin oil through which the moisturized C_3O_2 is passed. The reactor tube is heated in an oil bath to 130—135 °C. The volatile reaction products are passed through a cold-trap at −75 °C in which the less volatile fraction is collected, such as the acid components CH_3COOH etc. The volatile fraction is then trapped with liquid nitrogen. This fraction consists mainly of C_3O_2 and a small amount of C_3OS. C_3O_2 and C_3OS can easily be separated due to the difference in vapour pressure — 70 °C. The C_3OS is further purified by a single-plate distillation from −80 °C into a sample tube at liquid nitrogen temperature. It is important for the purification that the contents of the C_3OS trap are repeatedly melted and recooled to dry ice temperature during the distillation process. In this way some impurities are kept back. Unreacted C_3O_2 is fed back into a C_3O_2 storage vessel. The yield of this process is extremely low. Only about 0.2% of C_3O_2 is converted into C_3OS at each pass. In order to improve the yield a cyclic procedure has been adapted as can be seen from Figure 1. It was found that for C_3OS at −78 °C the vapour pressure is about 0.08 mbar.

b) Microwave Measurements

The microwave spectrum of C_3OS was recorded using a Hewlett-Packard spectrometer model MRR 8460 A. The frequency range covered by this spectrometer is 8 to 40 GHz. All measurements were carried out at room temperature. The reproducibility of the reported frequencies is 10 to 20 kHz. The C_3OS sample showed about 15% decrease of the line intensities after several hours in the gold-plated absorption cell at a pressure of 0.025 mbar. The measurements were carried out at a sample pressure of 0.010 mbar. Since C_3OS is rather sensitive to the presence of water vapour in the absorption cell, we conditioned the cell for several hours with C_3O_2 which removed all traces of water very effectively.

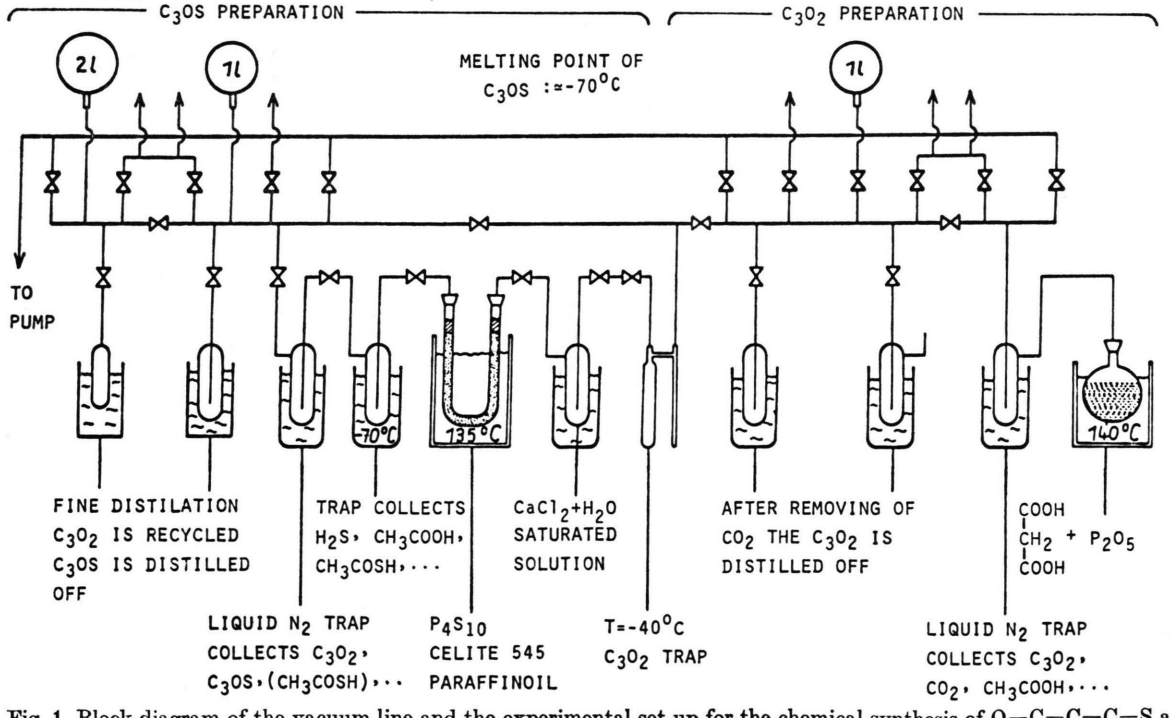

Fig. 1. Block diagram of the vacuum line and the experimental set-up for the chemical synthesis of O=C=C=C=S and its purification via distillation.

III. Spectral Data and Strategy for their Analysis

An overview of the $J = 11 \leftarrow 10$ rotational transition is shown in Figure 2. The vibrational satellite lines arising from the excitation of the ν_7 fundamental vibration can be followed very easily up to $\nu_7 = 9$ in Figure 2. The other, not specifically labeled, satellite lines arise from molecules in the other two bending states, ν_5 and ν_6, and their combination states with ν_7, $2\nu_7$, etc. In Figs. 3—7 expanded segments of the same spectrum are shown with the assignment of the lines. As can be clearly seen from the figures, the higher the excitation of the ν_7 vibration the more satellite lines occur in each group of lines which obviously belong together. These lines arise from substates which are coupled by l-type resonance interactions. The individual substates are distinguished by the vibrational angular momentum quantum number l. The data presented in this paper cover 11 rotational transitions from $J = 4 \leftarrow 3$ to $J = 14 \leftarrow 13$ which have been measured for $\nu_7 = 0$ to $\nu_7 = 7$, with $l = 0$ to $l = 6$ and for $\nu_5 = 1$ and $\nu_6 = 1$, with $l = 1$. Due to the small dipole moment of C_3OS of 0.662 Debye for the ground vibrational state the observed line width is about 150 kHz [7].

a) The Energy Matrix of a Linear Molecule

The Hamiltonian adopted for the analysis of the experimental data is based on the formalism developed by Nielsen [9, 10] and Amat and Nielsen [11]. This theory rests on three assumptions:

1) The equilibrium structure of the molecule is linear.
2) The amplitudes of the normal modes of vibration are small.
3) The potential function associated with each of the three bending modes of the C_3OS molecule may be represented by a two-dimensional isotropic harmonic oscillator with slight anharmonicity.

The unperturbed rovibrational energy E_{RV} which results when some of the larger effects of anharmonicity are included in the Hamiltonian may be approximately expressed by the diagonal matrix element [12]. The analytical expression of the diagonal matrix element is reduced for this discussion to the case in which only one bending mode, for example ν_7, is excited:

$$\langle v_t, l_t | \hat{H} | v_t, l_t \rangle = (E_{\text{Vib}} + E_{\text{Rot}}), \qquad (1)$$

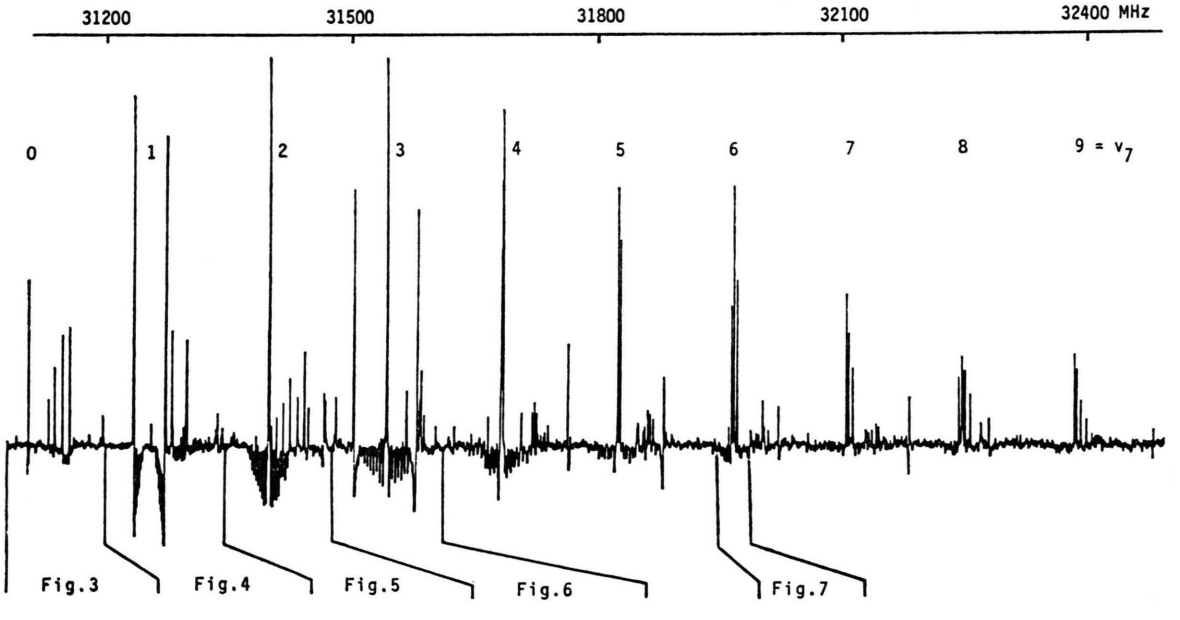

Fig. 2. Survey scan of the $J = 11 \leftarrow 10$ rotational transition as observed with a hp MRR 8460 spectrometer, showing the vibrational satellite lines dominated by those arising from energy levels of the vibrational manifold of the lowest lying bending mode ν_7.

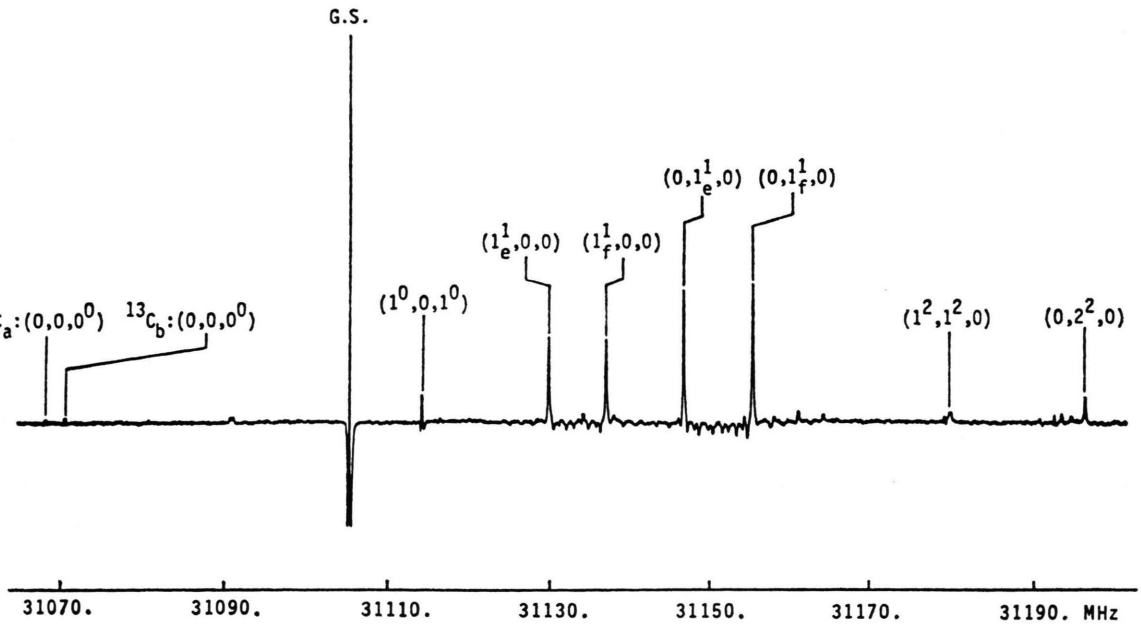

Fig. 3. Expanded scan of a portion of the spectral region shown in Figure 2. The ground state line and vibrational satellites are indicated. The l-type doublets of ν_5 and ν_6 can be clearly recognized. $^{13}C_a$ is 1—^{13}C and $^{13}C_b$ is 2—^{13}C of O=C=C=C=S.

where

$$E_{\mathrm{Vib}} = E_0^* + \omega_t(v_t + 1) + x_{tt}(v_t + 1)^2 + x_{l_t l_t} l_t^2, \quad (2)$$

$$E_{\mathrm{Rot}} = [B_v + \gamma_{l_t l_t} l_t^2][J(J+1) - l^2] - D_v[J(J+1) - l^2]^2 + H_v[J(J+1) - l^2]^3 \quad (3)$$

with

$$B_v = B_e^* - \alpha_t(v_t + 1) + \gamma_{tt}(v_t + 1)^2, \quad (4)$$

$$D_v = D_e^* + \beta_t(v_t + 1), \quad (5)$$

where

E_0^* the zero point energy of the other normal modes;

ω_t the harmonic frequency for the t-th normal mode;

x_{tt} anharmonicity constant for v_t in the expansion of the vibrational energy;

$x_{l_t l_t}$ anharmonicity constant which describes the contribution of the vibrational angular momentum l_t to the vibrational energy;

B_e^*, D_e^* effective equilibrium spectroscopic constants which include the zero point vibration contributions of the other normal modes;

B_v rotational constant for a given vibrational state;

α_t, β_t, γ_{tt} rovibrational interaction constants for the t-th normal mode;

$\gamma_{l_t l_t}$ rovibrational interaction constant;

D_v, H_v centrifugal stretching constants;

l sum of the vibrational angular momentum quantum numbers which in this case is $l = l_t$.

All the spectroscopic constants appearing in the expression for the rotational energy (3) and the expansion of the constants B_v (4) and D_v (5) as well as the anharmonicity constant $x_{l_t l_t}$ may be obtained from the rotational spectrum. For a given J, the energy difference between l sublevels may be seen from (2) and (3) to be given by

$$g_{l_t l_t} l^2 = (x_{l_t l_t} - B_v - \gamma_{l_t l_t} l_t^2 - D_v l^2 - H_v l^4) l^2 \cong (x_{l_t l_t} - B_v) l^2. \quad (6)$$

Using the second order transformed Hamiltonian [11], only states of different l but with the same v and J are connected by off-diagonal matrix elements of which the most important matrix elements

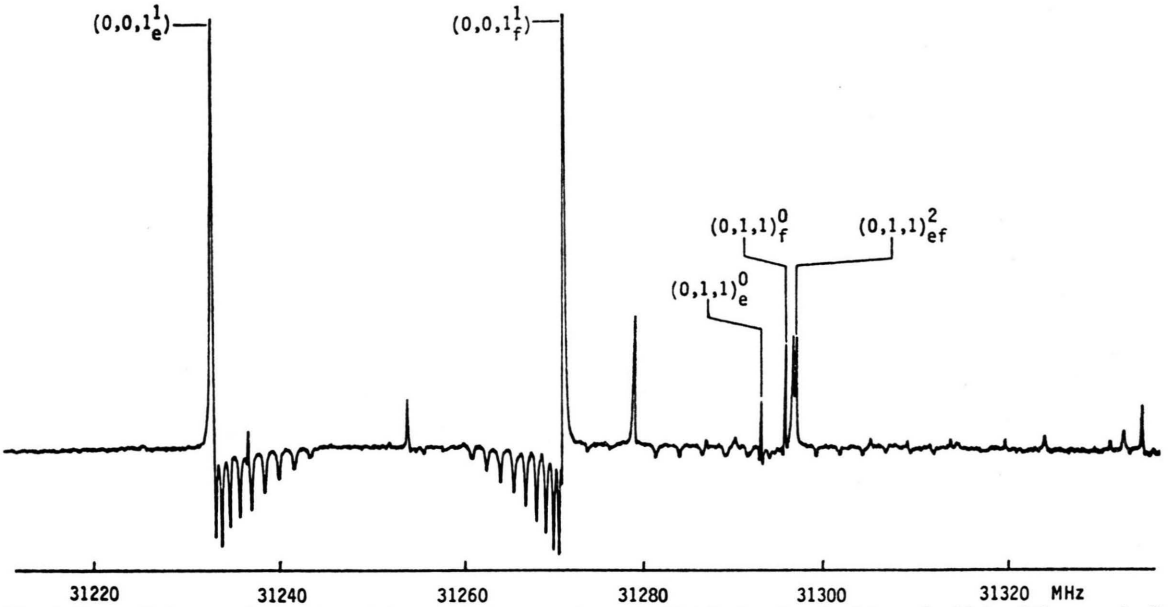

Fig. 4. Expanded scan of a portion of the spectral region shown in Fig. 2, showing the l-type doublets of the $v_7 = 1$ vibrational state.

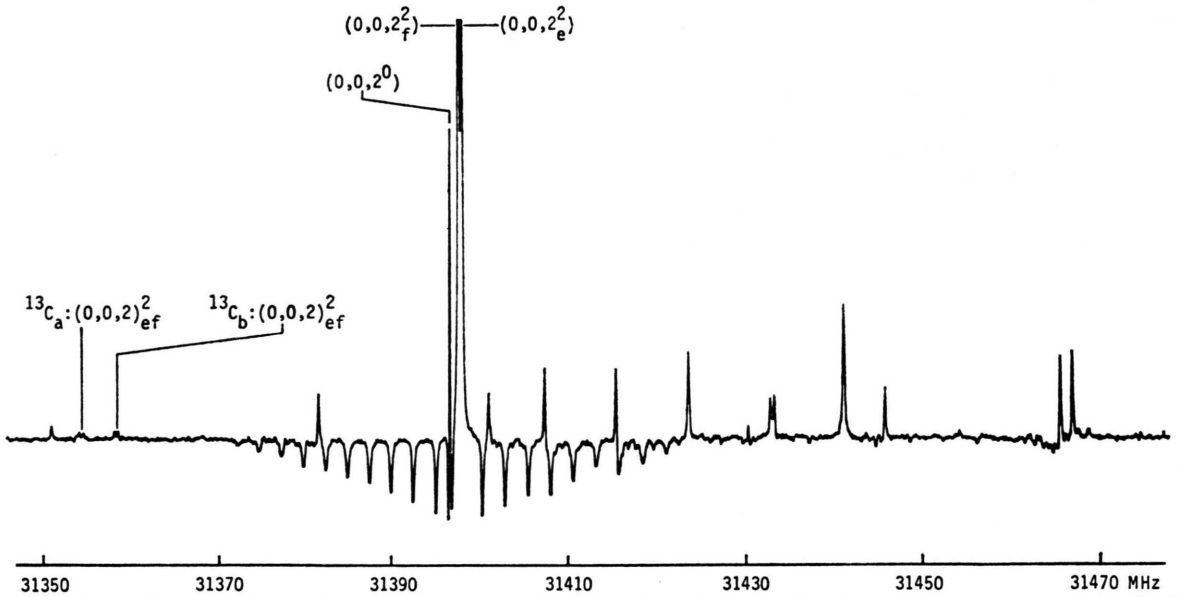

Fig. 5. Expanded scan of a portion of the spectral region shown in Fig. 2, showing the $v_7 = 2$ l-type resonance multiplet. $^{13}C_a$ is 1—^{13}C and $^{13}C_b$ is 2—^{13}C of O=C=C=C=S.

are of the type*

$$\langle v_t, l_t | \hat{H}_2' | v_t, l_t \pm 2 \rangle = \frac{q_t}{4} \{(v_t \mp l_t)(v_t \pm l_t + 2) \cdot [J(J+1) - l(l \pm 1)] \cdot [J(J+1) - (l \pm 1)(l \pm 2)]\}^{1/2}, \quad (7)$$

and has been discussed in detail in [12]. This type of matrix element contributes to every excited state $v_t > 0$. We can neglect the higher order interactions expressed by higher order matrix elements

* The phase factor taken here is different from that taken in Ref. [10, 19] and results in a positive off-diagonal matrix element, and thus a positive definition of q_t.

as discussed in Ref. [12] in the case of the present data, though we did find it necessary to include the J-dependence of q_7:

$$q_7 = q_7^{(0)} - q_7^{(1)} J(J+1). \tag{8}$$

From a theoretical point of view the discussion of the energy levels belonging to these vibrational states is straightforward. However, in practice the size of the energy matrix and the number of matrix elements becomes large with increasing v. For that reason we developed a fitting program which can handle in a systematic way the l-type resonance in any vibrational state for a single bending mode in a linear molecule, limited only by the array size in the program.

The analysis was approached by exploiting the analogy between the energy matrix of a linear molecule in various excited states of a single bending mode and that of an asymmetric rotor molecule in a single vibrational state. The angular momentum quantum number l in the former case and $K = K_a$ in the latter case are equivalent [10, 13]; the overall parity + or − of the rovibrational states has the same meaning in both types of molecules [14] and the correlation between the associated energy levels has been discussed frequently [4]. The off-diagonal matrix elements are only $\Delta l = \pm 2$ in the former case, and only $\Delta K = \pm 2$ in the latter case (at least in the A reduction of the Hamiltonian [15]), and even have the same J and K dependence [16, 17]. Therefore, the method and notation used in the analysis of an asymmetric rotor spectrum was applied in the organization of a fitting program for the analysis of the present C_3OS data.

There is a separate energy matrix for each vibrational quantum number v and for each rotational quantum number J. Each block of the energy matrix is of size $(v+1) \times (v+1)$ and tridiagonal. The energy matrix for even v is called $|\hat{E}|$ and is composed only of even-l basis functions, just as the even-K submatrix of an asymmetric rotor [17]. Similarly, the energy matrix for the odd vibrational states is composed of only odd-l basis functions and is called $|\hat{O}|$, in analogy to the odd-K submatrix of an asymmetric rotor [17].

b) The Wang Transformation and the Symmetry of Rovibrational Energy Levels

Since the energy matrices thus obtained have the same forms as those of an asymmetric rotor, they can be further factorized into two submatrices by applying a Wang transformation of the basis functions:

$$\Psi^{\pm}(v, J, |l|) = [|v, J, |l|\rangle \pm |v, J, -|l|\rangle]/\sqrt{2} \tag{9}$$

for $l \neq 0$, and

$$\Psi^{+}(v, J, 0) = |v, J, 0\rangle, \tag{10}$$

where $|v, J, \pm|l|\rangle$ is the basis wavefunction of a linear molecule, and $\Psi^{\pm}(v, J, |l|)$ is the transformed wavefunction. The transformed matrices after rearranging the rows and columns are the submatrices $|\hat{E}|^{+}$, $|\hat{E}|^{-}$, $|\hat{O}|^{+}$, $|\hat{O}|^{-}$. Since these submatrices are the same as those of an asymmetric rotor the reader is referred to the detailed discussion by Gordy and Cook [17] where the explicit form of the matrices is given.

In our choice of the phase factor of the basis wavefunction, the symmetry of the wavefunction $\Psi^{\pm}(v, J, |l|)$ is obtained* as listed in Table 1, where the correspondence among symmetry designations for wavefunctions, energy submatrices and energy levels is summarized. When the l-type coupling constant q_t is positive, as is generally the case for linear molecules, an eigenvalue of the $|\hat{O}|^{+}$ matrix, an **f** state [18], corresponds to the upper component (U) of an l-type doublet. An eigenvalue of the $|\hat{O}|^{-}$ matrix, an **e** state, corresponds to the lower component (L). The opposite is the case if the constant q_t is negative. The use of the **e** and **f** notation included in Table 1 has been recommended by Brown et al. [18].

On the other hand, the symmetry of the levels of even v, the eigenstates of the $|\hat{E}|^{\pm}$ matrices, cannot be correlated simply to upper and lower components of the l-type resonance doublets. As discussed in detail in Ref. [12], the symmetry has to be identified by finding a relation between the level in question and an $l = 0$ level, which is an **e** state for a $^1\Sigma^+$ vibronic state and an **f** state for a $^1\Sigma^-$ vibronic state. Such a procedure of symmetry identification has to be used also for an odd v state if a rigorously unambiguous classification of the level is needed, rather than the above correspondence based on assuming the sign of q. For an $l = 1$ state the unambiguous assignment is possible by observing an $l = 0 \rightarrow l = 1$ transition, or by observing an accidental resonance between an $l = 0$ and an $l = 1$ state.

Sub-matrix	l	γ	Parity		EPI Group Symmetry[a]		State Index[b]	l-Doublet Comp.[c]	
			J even	J odd	J even	J odd			
								$g_{l_t l_t} > 0$	$g_{l_t l_t} < 0$
$\lvert\hat{E}\rvert^+$	even	+	+	−	Σ^+	Σ^-	e	U	L
$\lvert\hat{E}\rvert^-$	even	−	−	+	Σ^-	Σ^+	f	L	U
								$q_t > 0$	$q_t < 0$
$\lvert\hat{O}\rvert^+$	odd	+	−	+	Σ^-	Σ^+	f	U	L
$\lvert\hat{O}\rvert^-$	odd	−	+	−	Σ^+	Σ^-	e	L	U

Table 1. Symmetry Classification of the Wavefunction $\Psi^\gamma(v, J, l)$ and Submatrices of Excited States of a Single Bending Mode of a Linear Molecule in a $^1\Sigma^+$ Electronic State.

[a] Notation recommended by Bunker and Papousek [14]. [b] Notation recommended by Brown et al. [18].
[c] Lower and upper component of the l-type doubling are indicated by L and U, respectively rather than **a** and **b** as suggested in Ref. [18], because **a** and **b** are often used to indicate the symmetry for C_2.

IV. Assigment and Analysis of C_3OS Data

a) Assignment

For an odd v state, the $l=1$ level splits into two well-separated substates of symmetry species **e** and **f** due to the off-diagonal matrix element given in (7). This correction to the energy is the largest among the various vibration-rotation corrections, since the substates are otherwise degenerate and the correction is a first-order correction. Therefore, we can assign the levels with the aid of the relations given in Table 1 for $|\hat{O}|$ submatrices assuming $q_7 > 0$. For even v states, the $l=2$ substate splits into **e** and **f** substates, which can be assigned as follows: When $g_{l_t l_t}$ is positive the $l=2$ level is higher in energy than the $l=0$ level. Thus the **e** component of the $l=2$ state is pushed up by the l-type resonance interaction. Similarly, when the constant $g_{l_t l_t}$ is negative, the **e** energy level is pushed down. Thus the **e** level is higher than the **f** level for $g_{l_t l_t} > 0$, and vice versa, as listed in Table 1. The corrections discussed for the $|l|=1$ or $|l|=2$ states propagate into higher $|l|$ eigenvalues, as in an asymmetric rotor. The relations given in Table 1 are valid except when accidental perturbations are present. It is not necessary in the present data to distinguish **e** and **f** in the $|l| \geqq 3$ substates, because the energy separation is very small and cannot be detected under Doppler resolution in the frequency range covered.

Since the sign of the constant $g_{l_t l_t}$ was not known, we had to extract this information from the effects of the l-type resonance in order to identify the **e** and **f** components in the observed spectrum. The δ-plot [19] is helpful in this respect. The quantity δ is defined for a pure rotational transition in a given (v, l) state as

$$\delta = \frac{\nu}{2(J+1)} - B_{v,l} + 2D_0(J+1)^2, \quad (11)$$

where $B_{v,l}$ is the effective rotational constant for the excited state obtained by fitting all the data for a given v, l component to the expression

$$\nu = 2(J+1)B_{v,l} - 4(J+1)^3 D_{v,l}, \quad (12)$$

and D_0 is the centrifugal distortion constant in the ground vibrational state. This quantity represents the deviation of the effective centrifugal distortion contribution in an excited vibrational state from that in the unperturbed case, represented by the ground vibrational state. An example of the δ plot for the $v=6$ state of C_3OS is shown in Figure 8. The $l=0$ substate and the upper component of the $l=2$ state show large, symmetrical shifts relative to the vertical which indicate that these levels are coupled by the l-type resonance interaction. Since only levels of the same rovibrational symmetry can be coupled, we can conclude that the $l=0$ and $l=2_U$ levels are of the same symmetry and can thus be labeled **e**. In addition we may conclude that $g_{l_t l_t}$ is positive for this particular system of interacting levels.

b) Least Squares Analysis of the Measured Lines

The measured vibrational satellite lines collected in Table 2 are R-branch transitions for which $\Delta J = +1$ and $\Delta l = 0$. The structure of the non-linear least squares fitting program is modelled after our asymmetric rotor programs. The quantum numbers and symmetry assignments are used to select the appropriate energy levels from the submatrix eigenvalues. The program sets up the Jacobian matrix, which is the derivative of the energy with respect

Table 2. Observed Rotational Frequencies of C_3OS in MHz and Deviations from the Calculated Frequencies for the Vibrational States Indicated by (v_5^l, v_6^l, v_7^l).

$J+1 \leftarrow J$	(0, 0, 0)		$(1_e^1, 0, 0)$		$(1_f^1, 0, 0)$		$(0, 1_e^1, 0)$	
	ν_{obs}	O–C	ν_{obs}	O–C	ν_{obs}	O–C	ν_{obs}	O–C
4 ← 3	11311.284	− 0.004	11320.204	0.013	11322.759	− 0.017	11326.258	0.009
5 ← 4	14139.110	0.008	14150.232	0.001	14153.461	− 0.001	14157.819	0.016
6 ← 5	16966.913	0.002	16980.271	0.007	16984.133	− 0.009	16989.366	0.013
7 ← 6	19794.703	− 0.010	19810.302	0.011	19814.809	− 0.006	19820.889	− 0.007
8 ← 7	22622.513	0.004	22640.300	− 0.010	22645.479	− 0.001	22652.428	− 0.004
9 ← 8	25450.292	− 0.003	25470.308	− 0.012	25476.135	− 0.001	25483.953	− 0.007
10 ← 9	28278.074	0.002	28300.316	− 0.003	28306.793	0.011	28315.472	− 0.007
11 ← 10	31105.845	0.006	31130.306	− 0.001	31137.425	0.009	31146.995	0.008
12 ← 11	33933.587	− 0.007	33960.295	0.012	33968.049	0.011	33978.469	− 0.016
13 ← 12	36761.341	0.005	36790.239	− 0.006	36798.639	− 0.007	36809.979	0.009
14 ← 13	39589.063	− 0.002	39620.191	− 0.001	39629.234	− 0.005	39641.442	0.001

$J+1 \leftarrow J$	$(0, 1_f^1, 0)$		$(0, 0, 1_e^1)$		$(0, 0, 1_f^1)$		$(0, 0, 2^0)$	
	ν_{obs}	O–C	ν_{obs}	O–C	ν_{obs}	O–C	ν_{obs}	O–C
4 ← 3	11329.308	− 0.015	11357.422	0.006	11371.413	− 0.006	11417.134	0.011
5 ← 4	14161.636	− 0.010	14196.769	0.008	14214.271	0.007	14271.378	− 0.001
6 ← 5	16993.953	− 0.011	17036.102	0.003	17057.094	− 0.008	17125.628	0.010
7 ← 6	19826.280	0.005	19875.427	− 0.002	19899.942	0.010	19979.836	− 0.001
8 ← 7	22658.583	0.003	22714.746	− 0.004	22742.751	− 0.002	22834.039	0.006
9 ← 8	25490.876	0.000	25554.050	− 0.011	25585.553	− 0.010	25688.212	0.010
10 ← 9	28323.175	0.011	28393.371	0.011	28428.369	0.009	28542.345	0.004
11 ← 10	31155.440	− 0.001	31232.632	− 0.014	31271.148	0.003	31396.446	− 0.001
12 ← 11	33987.716	0.010	34071.925	0.007	34113.916	0.001	34250.513	− 0.003
13 ← 12	36819.959	− 0.001	36911.176	0.001	36956.658	− 0.011	37104.539	− 0.006
14 ← 13	39652.194	− 0.006	39750.415	0.001	39799.410	0.005	39958.519	− 0.011

$J+1 \leftarrow J$	$(0, 0, 2_e^2)$		$(0, 0, 2_f^2)$		$(0, 0, 3_e^1)$		$(0, 0, 3_f^1)$	
	ν_{obs}	O–C	ν_{obs}	O–C	ν_{obs}	O–C	ν_{obs}	O–C
4 ← 3	11417.354	− 0.012	11417.354	0.006	11455.436	0.001	11483.736	0.003
5 ← 4	14271.683	− 0.025	14271.683	0.010	14319.279	0.003	14354.650	0.002
6 ← 5	17126.015[a]	− 0.037	17126.015[a]	0.025	17183.110	0.006	17225.541	− 0.009
7 ← 6	19980.340[a]	− 0.056	19980.340[a]	0.042	20046.915	− 0.003	20096.435	− 0.002
8 ← 7	22834.734	− 0.008	22834.594	− 0.001	22910.723	0.007	22967.307	0.001
9 ← 8	25689.055	− 0.034	25688.907	0.028	25774.485	− 0.009	25838.149	− 0.006
10 ← 9	28543.429	− 0.010	28543.157	0.008	28638.235	− 0.015	28708.988	0.007
11 ← 10	31397.788	0.000	31397.403	0.001	31501.991	0.009	31579.787	0.004
12 ← 11	34252.134	− 0.007	34251.647	0.008	34365.695	0.007	34450.565	0.009
13 ← 12	37106.495	0.000	37105.860	0.003	37229.363	− 0.003	37321.290	− 0.010
14 ← 13	39960.859	0.008	39960.058	0.005				

$J+1 \leftarrow J$	$(0, 0, 3_{ef}^3)$		$(0, 0, 4^0)$		$(0, 0, 4_e^2)$		$(0, 0, 4_f^2)$	
	ν_{obs}	O–C	ν_{obs}	O–C	ν_{obs}	O–C	ν_{obs}	O–C
4 ← 3	11470.067	0.008	11521.467	0.014	11521.785[a]	− 0.037	11521.785[a]	0.021
5 ← 4	14337.577	0.011	14401.768	0.011	14402.241[a]	− 0.059	14402.241[a]	0.057
6 ← 5	17205.060	− 0.008	17282.036	0.014	17282.700[a]	− 0.094	17282.700[a]	0.109
7 ← 6	20072.555	− 0.008	20162.236	− 0.004	20163.289	− 0.018	20162.999	0.017
8 ← 7	22940.053	0.002	23042.408	0.005	23043.821	− 0.021	23043.367	0.013
9 ← 8	25807.532	0.002	25922.503	0.000	25924.373	− 0.028	25923.732	0.027
10 ← 9	28674.998	− 0.002	28802.530	− 0.002	28804.985	− 0.003	28804.035	0.004
11 ← 10	31542.454	− 0.006	31682.482	− 0.001	31685.606	0.000	31684.331	0.001
12 ← 11	34409.914[b]	0.007	34562.344	− 0.003	34566.260	0.002	34564.596	− 0.003
13 ← 12	37277.342[b]	0.000	37442.109	− 0.009	37446.953	0.006	37444.831	− 0.005

Table 2 continued.

$J+1 \leftarrow J$	$(0,0,4^4_{ef})$		$(0,0,5^1_e)$		$(0,0,5^1_f)$		$(0,0,5^3_{ef})$	
	ν_{obs}	O–C	ν_{obs}	O–C	ν_{obs}	O–C	ν_{obs}	O–C
4 ← 3			11551.699	0.012	11594.528	0.005	11573.678	− 0.009
5 ← 4	14403.151	− 0.009	14439.593	0.014	14493.140	0.019	14467.090	− 0.011
6 ← 5	17283.763	− 0.013	17327.463	0.013	17391.707	0.010	17360.491	− 0.020
7 ← 6	20164.383	− 0.001	20215.302	0.005	20290.256	0.009	20253.902	− 0.013
8 ← 7	23044.977	− 0.005	23103.117	0.002	23188.774	0.008	23147.304	− 0.007
9 ← 8	25925.564	− 0.005	25990.899	− 0.003	26087.248	− 0.002	26040.695[b]	− 0.006
10 ← 9	28806.149	0.006	28878.659	0.007	28985.698	0.003	28934.076[b]	− 0.006
11 ← 10	31686.708	0.005	31766.364	0.002	31884.095	− 0.001	31827.451[b]	− 0.002
12 ← 11	34567.252	0.005	34654.023	− 0.005	34782.439	− 0.009	34720.809[b]	− 0.004
13 ← 12	37447.780	0.005	37541.642	− 0.004	37680.748	0.000	37614.168[b]	0.006

$J+1 \leftarrow J$	$(0,0,5^5_{ef})$		$(0,0,6^0)$		$(0,0,6^2_e)$		$(0,0,6^2_f)$	
	ν_{obs}	O–C	ν_{obs}	O–C	ν_{obs}	O–C	ν_{obs}	O–C
5 ← 4			14529.957	0.023	14530.658[a]	− 0.111	14530.658[a]	0.138
6 ← 5	17362.125	− 0.002	17435.769	0.012	17436.998	− 0.015	17436.609	0.031
7 ← 6	20255.789	0.000	20341.499	0.008	20343.298	− 0.008	20342.623	0.013
8 ← 7	23149.438	− 0.001	23247.140	0.020	23249.655	− 0.002	23248.624	0.011
9 ← 8	26043.072	− 0.004	26152.647	0.017	26156.078	0.004	26154.592	0.009
10 ← 9	28936.698	0.000	29058.022	0.015	29062.577	0.013	29060.517	0.002
11 ← 10	31830.306	0.003	31963.253	0.018	31969.135	0.000	31966.403	− 0.002
12 ← 11	34723.889	0.000	34868.312	0.011	34875.815	0.018	34872.239	− 0.009
13 ← 12	37617.470	0.015	37773.177	− 0.012	37782.586	0.031	37778.056	0.014

$J+1 \leftarrow J$	$(0,0,6^4_{ef})$		$(0,0,6^6_{ef})$	
	ν_{obs}	O–C	ν_{obs}	O–C
5 ← 4	14531.622	− 0.025		
6 ← 5	17437.932	− 0.029		
7 ← 6	20344.235	− 0.032	20346.761	0.018
8 ← 7	23250.523	− 0.041	23253.406	0.022
9 ← 8	26156.813	− 0.036	26160.021	0.011
10 ← 9	29063.080	− 0.042	29066.636	0.018
11 ← 10	31969.337	− 0.044	31973.227	0.018
12 ← 11	34875.560	− 0.066	34879.803	0.024
13 ← 12	37781.812	− 0.041	37786.351	0.025

$J+1 \leftarrow J$	$(0,0,7^1_e)$		$(0,0,7^1_f)$	
	ν_{obs}	O–C	ν_{obs}	O–C
8 ← 7	23291.801	0.001	23406.907	0.001
9 ← 8	26203.119	− 0.001	26332.586	− 0.001

$J+1 \leftarrow J$	$(0,0,7^3_{ef})$		$(0,0,7^5_{ef})$	
	ν_{obs}	O–C	ν_{obs}	O–C
8 ← 7	23351.041[b]	− 0.002	23353.254	0.001
9 ← 8	26269.913[b]	0.001	26272.363	− 0.001

[a] Lines not used in fit due to unresolved doublet.
[b] Calculated splitting due to *l*-type resonance interaction 2 to 13 kHz. Therefore, the average value of the calculated line positions was used in determining O–C.

to the molecular parameters, via the Hellman-Feynman theorem [20],

$$\frac{\partial \varepsilon}{\partial \lambda} = \int \Psi^* \frac{\partial \hat{H}}{\partial \lambda} \Psi \, d\tau, \tag{13}$$

where $\hat{H}\Psi = \varepsilon\Psi$, and λ is one of the molecular parameters.

This fast and compact method has been used with success in our programs for the centrifugal distortion analysis of asymmetric rotor spectra. The matrix diagonalisation section of the program utilizes the Rutishauser-procedure [21] while the linear least squares subroutine and error calculations are standard. The entire procedure is iterated until a convergence is reached.

The adjusted constants for C_3OS in the successive vibrational states of the ν_7 bending mode and the first excited states of ν_5 and ν_6 are given in Table 3. Using these constants the values of the frequencies of the transitions given in Table 2 were calculated.

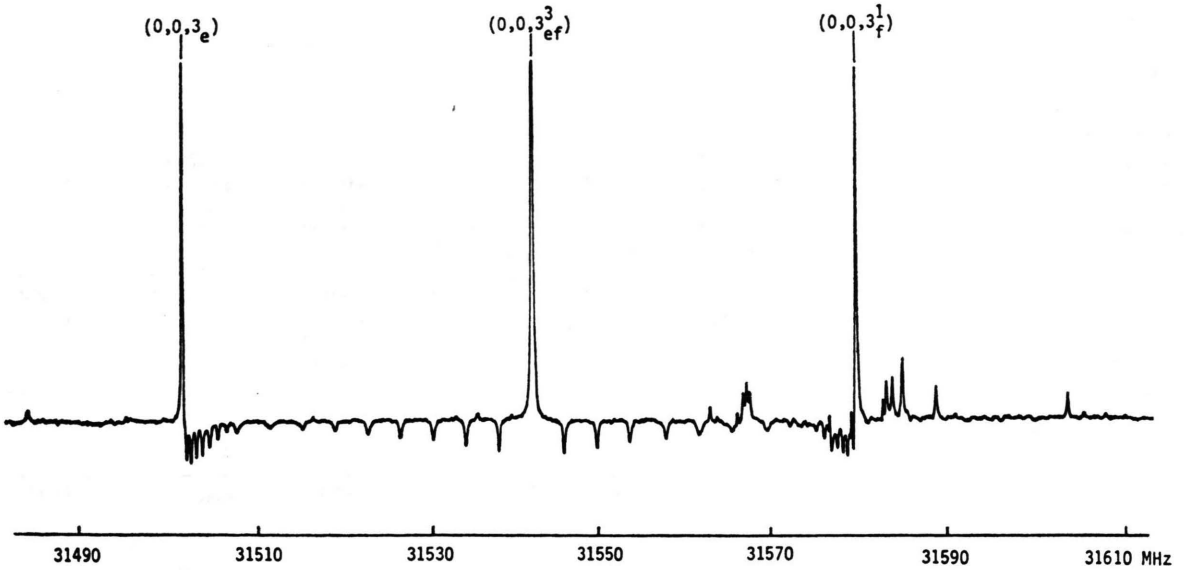

Fig. 6. Expanded region of a portion of the spectral region shown in Fig. 2, showing the $v_7 = 3$ satellite lines. $(0, 0, 3_e)$ should read $(0, 0, 3_e^1)$.

Table 3. Spectroscopic Constants of C_3OS in Excited Vibrational States.

(v_5, v_6, v_7)	B_{v_t}/MHz	D_{v_t}/Hz	$q_{v_t}^{(0)}$/MHz	$q_{v_t}^{(1)}$/Hz	$\gamma_{l_t l_t}$/kHz	$x_{l_t l_t}$/cm^{-1}	σ/KHz[b]
(0, 0, 0)	1413.91242 (25)	43.98 (91)					6.1
(0, 0, 1)	1420.54876 (23)	54.84 (85)	1.75041 (47)	1.90 (171)	5.30[a]		8.1
(0, 0, 2)	1427.14471 (40)	65.95 (116)	1.75952[a]	1.99[a]	6.346 (103)	0.4007 (41)	12.4
(0, 0, 3)	1433.69383 (27)	73.19 (87)	1.76872 (24)	2.07 (100)	7.098 (50)	0.3793 (99)	7.3
(0, 0, 4)	1440.19162 (33)	85.75 (124)	1.77600[a]	2.72[a]	7.816 (18)	0.3742 (9)	11.6
(0, 0, 5)	1446.63449 (22)	95.26 (82)	1.78496 (19)	4.31 (80)	8.419 (10)	0.3799 (19)	8.8
(0, 0, 6)	1453.02344 (61)	103.23 (241)	1.79248[a]	6.84[a]	8.800 (17)	0.3587 (9)	25.2
(0, 0, 7)	1459.35934 (46)	114.69 (311)	1.79989 (36)	10.30 (246)	8.926 (10)	0.3637 (12)	2.8
(0, 1, 0)	1415.97451 (28)	42.63 (102)	0.38424 (22)				9.7
(1, 0, 0)	1415.18691 (26)	47.41 (96)	0.32312 (10)				9.1

[a] Values interpolated or extrapolated and held fixed in fit. [b] Standard deriation of the fit.

Table 4. Parameters obtained by fitting the Spectroscopic constants given in Table 3 to a power series Expansion in $(v + 1)$

$B^*_{7(e)}$[a]	= 1407.2298 (48) MHz	$\gamma^*_{l_7 l_7(e)}$ =	2.791 (289) kHz	$D^*_{7(e)}$ =	34.75 (89) Hz
$B_{7(1)} = -\alpha_7$ =	6.7018 (43) MHz	$\gamma_{l_7 l_7(1)}$ =	1.411 (112) kHz	$D_{7(1)} = \beta_7$	9.97 (18) Hz
$B_{7(2)} = \gamma_{77}$ =	−0.01984 (109) MHz	$\gamma_{l_7 l_7(2)}$ =	− 0.080 (10) kHz		
$B_{7(3)}$ =	−0.422 (80) kHz				
$q^{(0)*}_{7(e)}$ =	1.73483 (147) MHz	$q^{(1)*}_{7(e)}$ =	− 5.06 (105) Hz[a]	$x^*_{l_7 l_7(e)}$ =	0.4140 (111) cm^{-1}
$q^{(0)}_{7(1)}$ =	0.008234 (269) MHz	$q^{(1)}_{7(1)}$ =	2.27 (48) Hz	$x_{l_7 l_7(1)}$ =	− 0.0069 (19) cm^{-1}
		$q^{(1)}_{7(2)}$ =	− 0.364 (47) Hz		

[a] The power series expansion in terms of $(v_7 + 1)$ may not be physically applicable for $q_7^{(1)}$.

V. Discussion

The adjusted spectroscopic constants of C_3OS collected in Table 3 are representative for a well-behaved linear molecule. The l-type doubling constant is assumed positive for all three bending modes*. The rotational constants B_v and D_v can be expanded according to (4) and (5) and the results of a fit to the (equally weighted) values of B_{v_7} and D_{v_7} are given in Table 4. A similar expansion of several of the other molecular parameters as a function of vibrational quantum number v_7

$$P_t = P^*_{t(e)} + P^*_{t(v)}(v_7 + 1) + \ldots \qquad (14)$$

is necessary and the results of the corresponding fits are also given in Table 4. The variation of $q_7^{(1)}$ with v is not well determined and not clearly linear. It should be pointed out that the sign of $x_{l_7 l_7}$ is positive, and $x_{l_i l_i}$ is much larger than B_v for all reported states. This means that the higher l-substates lie at successively higher energy. Only a small decrease of the magnitude of the constant $x_{l_7 l_7}$ can be observed with increasing v_7. In the $v_7 = 6$ state systematic deviations are observed in the least squares fit; the variation of $B_{v,l}$ with l no longer goes as l^2 as could be seen clearly from survey scans for $v_7 > 7$. A trial fit with an l^4 correction to B_v reduced the deviations for $v_7 = 6$ and changes the parameters $\gamma_{l_i l_i}$ and $x_{l_i l_i}$ slightly. However, since this term is determined only for $v_7 = 6$ and no precision measurments have yet been made for $v_7 > 7$ or $l > 6$ this term has not been included in the analysis presented here.

The positive sign of $x_{l_7 l_7}$ and its small dependence on the vibrational quantum number v_7 imply a rather harmonic bending potential function for v_7. The vibrational energy levels must then be equidistant. A forthcoming publication [7, 22] will report our determination of the vibrational term values of the v_7 vibrational manifold whose fundamental was found to be 82.9 cm^{-1}. Of course, these results are in sharp contrast to the quasilinearity of C_3O_2 [2, 5] whose lowest lying fundamental vibration was found to be 18.2 cm^{-1} [3].

Long linear carbon chain molecules have rather flexible structures with low — lying, large — amplitude bending states which are well populated at room temperature. Recently Hutchinson, Kroto and Walton [23] have studied cyanobutadiyne, H—CC—CC—CN, and reported the analysis of the lowest lying vibrational manifold for which $\nu_{11} \cong 75$ cm^{-1}.

Acknowledgements

One of us (J. J. Chr.) would like to express his gratitude to the Physikalisch-Chemisches Institut der Justus-Liebig-Universität Giessen for the hospitality extended to him during the summer months of the years 1976 to 1979 where this work was carried out. The authors would like to express their sincere thanks to Dr. Brenda P. Winnewisser for many helpful discussions and critically reading and commenting on the manuscript.

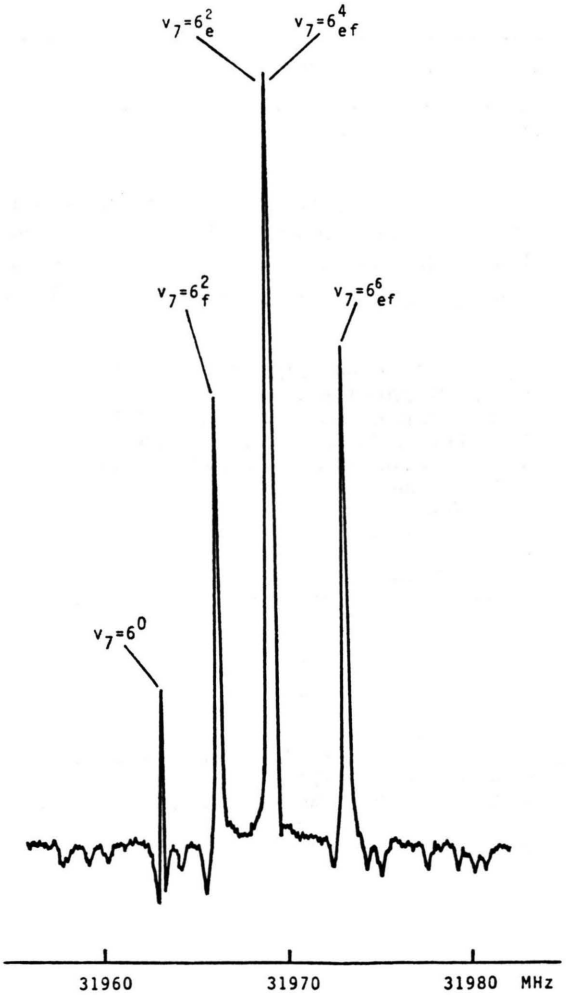

Fig. 7. Expanded region of a portion of the spectral region shown in Fig. 2, showing the $v_7 = 6$ l-type resonance polyade.

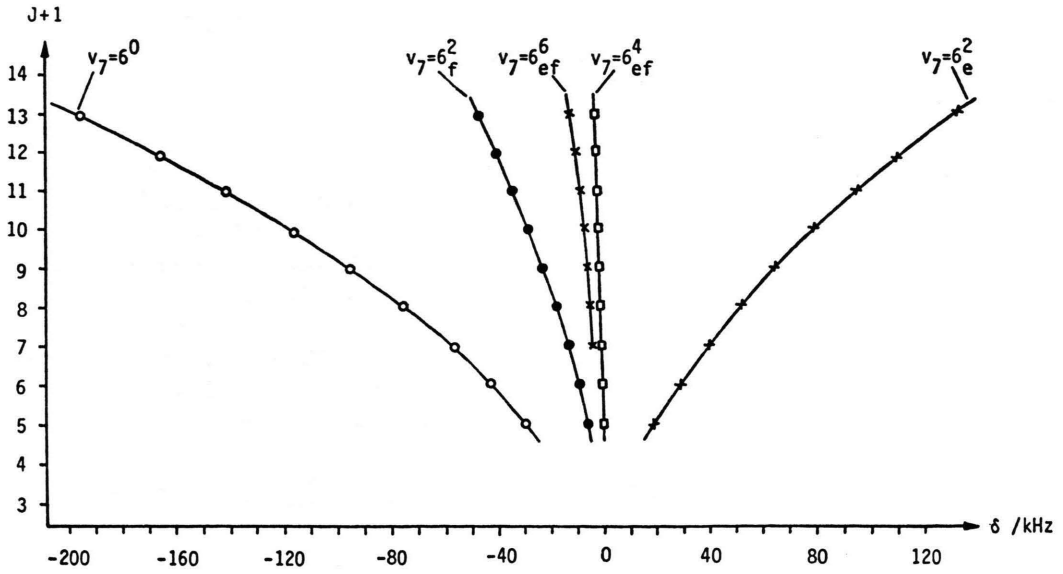

Fig. 8. The quantity δ (see text) is plotted as a function of $J+1$ showing clearly the interaction between states with like symmetry, 6^0 and 6_e^2, which are coupled by the l-type resonance.

The work was supported in part by funds from the Deutsche Forschungsgemeinschaft and the Fonds der Chemischen Industrie. The microwave spectrometer was made available by the Max-Planck-Institute für Radioastronomie through the grants of Dr. Gisbert Winnewisser, whose interest in this work is very much appreciated.

[1] M. Winnewisser and J. J. Christiansen, Chem. Phys. Letters, **37**, 270 (1976).
[2] W. H. Weber, J. Mol. Spectrosc. **79**, 396 (1980).
[3] A. V. Burenin, E. N. Karyakin, A. F. Krupnov, and S. M. Shapin, J. Mol. Spectrosc. **78**, 181 (1979).
[4] K. Yamada and W. Winnewisser, Z. Naturforsch. **31a**, 139 (1976).
[5] P. R. Bunker, J. Mol. Spectrosc. **80**, 422 (1980).
[6] F. M. Nicolaisen and J. J. Christiansen, J. Mol. Struct. **52**, 157 (1979).
[7] M. Winnewisser and W. Peau, to be published.
[8] M. Winnewisser and W. Peau, to be published.
[9] H. H. Nielsen, Phys. Rev. **60**, 794 (1941).
[10] H. H. Nielsen, "Molecular Spectra" in Handbuch der Physik **37/1**, 174 (1959).
[11] G. Amat and H. H. Nielsen, J. Mol. Spectrosc. **2**, 152 (1958); **2**, 163 (1958).
[12] M. Winnewisser and B. P. Winnewisser, J. Mol. Spectrosc. **41**, 143 (1972).
[13] J. T. Hougen, P. R. Bunker, and J. W. C. Johns, J. Mol. Spectrosc. **34**, 136 (1970).
[14] P. R. Bunker and D. Papousek, J. Mol. Spectrosc. **32**, 419 (1969).
[15] J. K. G. Watson, Aspects of Quartic and Sectic Centrifugal Effects on Rotational Energy Levels, in "Vibrational Spectra and Structure", J. R. Durig, ed.; Elsevier, Amsterdam 1977.
[16] G. W. King, R. M. Hainer, and P. C. Cross, J. Chem. Phys. **11**, 27 (1942).
[17] W. Gordy and R. L. Cook, Microwave Molecular Spectra, in "Chemical Applications of Spectroscopy", W. West, ed. Part II, Interscience Publishers, John Wiley & Sons, New York 1970.
[18] J. M. Brown, J. T. Hougen, K.-P. Huber, J. W. C. Johns, I. Kopp, H. Lefebvre-Brion, A. J. Merer, D. A. Ramsay, J. Rostas, and R. N. Zare, J. Mol. Spectrosc. **55**, 500 (1975).
[19] K. Yamada, B. P. Winnewisser, and M. Winnewisser, J. Mol. Spectrosc. **56**, 449 (1975).
[20] R. P. Feynman, Phys. Rev. **36**, 340 (1939).
[21] R. S. Martin and J. M. Wilkinson, Numerische Mathematik, **12**, 377 (1968).
[22] M. Winnewisser, Faraday Discussion 71/2, April 1981.
[23] M. Hutchinson, H. W. Kroto, and D. R. M. Walton, J. Mol. Spectrosc. **82**, 394 (1980).